Initial Interaction of Crystalline Al/Amorphous Si Bilayer during Annealing

Yonghao Zhao[1,2], Jiangyong Wang[1] and Eric J. Mittemeijer[1]
[1]Max Planck Institute for Metals Research,
Heisenbergstr. 3, D-70569 Stuttgart, Germany
[2]Materials Science and Technology Division, Los Alamos National Laboratory,
Los Alamos, NM-87545, U.S.A.

ABSTRACT

Initial interaction of a magnetron sputter deposited Al(100 nm, {111} fibre textured)/Si(150 nm, amorphous) bilayer, induced by isothermally annealing at 523 K for 60 min in a vacuum of 2.0×10^{-4} Pa, was studied by X-ray diffraction, Auger electron microscopy and focused-ion beam imaging techniques. Upon annealing, the crystalline Si had grown into the grain boundaries of the Al layer with a {111} texture, a crystallite size of approximate 12 nm and a tensile stress of +138 MPa. Simultaneously, the Al grains had grown into the Si layer from the original interface of the a-Si and Al sublayers with the lateral grain growth. The stress parallel to the surface of the Al layer had changed from +27 MPa to +232 MPa after annealing.

INTRODUCTION

In the last decades, interdiffusion and/or reactions between semiconductor and metal systems have been paid increasing attention not only in view of the practical applications in the microelectronic industry [1–3], but also because of great scientific interest. Si/Al system is an interesting example, because according to the thermodynamics for bulk materials, Si and Al do not form compounds and are rather immiscible [5]. For Si (amorphous)/Al (crystalline) bilayers, further written as a-Si/Al, various studies showed that the presence of Al layer lowers the crystallization temperature of a-Si significantly as compared to bulk a-Si [6-8]. *In situ* transmission electron microscopy observation on an a-Si/Al multilayer showed that, during annealing at 493 K, c-Si nucleates within the Al layers and penetrates the Al as the c-Si grows [9]. Annealing an a-Si/Al bilayer (623-773 K) showed that c-Si nucleates at the Si/Al interface and grows further into the Al layer until, finally, a continuous c-Si film has formed at the initial Al layer, resulting in a layer exchange [10]. More recently, we found that the layer exchange can occur at even lower annealing temperature (523 K) accompanied with the crystallization of amorphous Si [11]. An extensive analysis indicated that the largest gain in energy upon transformation is due to the crystallization of the amorphous Si [11]. However, this driving force contribution cannot explain why layer exchange occurs. The objective of this investigation is to study the initial interaction of the Al/Si bilayer.

EXPERIMENTAL DETAILS

The thermally oxidized, single crystalline Si wafers were used as substrates. Prior to deposition, the chamber was pumped down to 10^{-7} Pa, the substrate and the Al, Si targets (with purities of 99.999 wt.%) were cleaned by argon ion sputtering. Then, the direct current magnetron sputter deposition of Al(100 nm)/Si(150 nm) bilayer was carried out at room temperature under an input power of 100 W and an Ar working pressure of 4.0×10^{-1} Pa. The

sputter apparatus has two exchangeable targets, enabling the preparation of the Al/Si bilayer under vacuum in a single run. The prepared Al/Si bilayer was isothermally annealed at 523 K for 60 min in a vacuum of 2.0×10^{-4} Pa, then cooled in vacuum with a cooling rate of 2 K/min.

The microstructural evolutions upon annealing were characterized by X-ray diffraction (XRD) and focused-ion beam (FIB) imaging. The XRD measurements were performed on a Philips MRD diffractometer equipped with a Eulerian cradle, a copper tube operating at 1.8 kW and a secondary monochromator to select Cu K_α radiation. For phase analysis, continuous θ-2θ scan was used. For texture analysis, a ϕ step scan of the {111} reflection of the Al layers was performed at different specimen tilt angles ψ from 0° to 90°. For the determination of macrostress, crystallite size and microstrain, the Al {111} and Si {111} reflections at different ψ angles were recorded by θ-2θ step scan. The peak parameters were then determined using Philips Profit 1.0c software. The FIB imaging analysis was carried out on a FEI 200 XP FIB microscope. A Ga^+ ion beam was accelerated towards the target sample by a voltage of 30 keV for generating the secondary electron images. Elements Al and Si as well as Al crystallites with different crystallographic orientations can be clearly distinguished because they show different (channeling) contrasts in the secondary electron images.

The compositional analysis was performed at a JEOL 7830 scanning Auger microscope at a base pressure below 8.0×10^{-8} Pa. The samples were sputtered using an ion gun with 1 keV Ar^+ ion beams. The Al (1396 eV), Si (1621 eV) and O (507 eV) Auger electron signals as a function of the sputtering time were quantified by applying the relative elemental sensitivity factors: S_{Al} = 0.23, S_{Si} = 0.16 and S_O = 0.23, with respect to the Auger electron signal of pure Ag (356 eV), which all were measured under the same experimental conditions.

EXPERIMENTAL RESULTS

The XRD patterns of the prepared and annealed Al/Si bilayers, as well as of the 'bare' Si(510) substrate, are shown in figure 1(a). The XRD patterns of the Al/Si bilayers, after subtracting the XRD background as recorded from the Si(510) substrate, are shown in figure 1(b). The prepared Si sublayer is amorphous, evidenced by the a-Si broad scattering peak at about $2\theta = 27°$ (figure 1b). After annealing, the a-Si sublayer had partially crystallized into polycrystalline Si with a {111} texture, because I_{220}/I_{111} and I_{311}/I_{111} intensity ratios of the c-Si are much smaller than the standard values on the ICDD-JCPDS card (no. 27-1402). The Al sublayers in the prepared and annealed Al/Si bilayers exhibit a {111} fibre texture.

The Auger electron spectroscopy (AES) depth profiles of the prepared and annealed $Al/Si/SiO_2/Si(510)$ bilayers were shown in figure 2. The prepared bilayer has a sharp interface. After annealing, the interdiffusion between a-Si and Al layers occurred: the Al moved into Si layer and the Si moved into the Al layer through the original Al/Si interface.

Figures 3(a,b) show the cross-sectional FIB micrographs. For the prepared sample, the Al layer, the Si layer and the SiO_2 layer as well as the Al crystallites with different crystallographic orientations can be clearly distinguished (figure 3a). The Al layer was composed of columnar crystallites with the size ranges from tens to about 500 nm. After annealing, the interface between Si and Al layers turned rough. The Si grew into the grain boundaries of the Al layer and some of them grew up till to the surface of the Al layer (see the material of dark intensity at the cross-section of figure 3b). Simultaneously, the Al grains (the material of bright intensity at the cross-section in figure 3b) grew downwards into the Si layer in a wedged shape and grew laterally into about several hundreds nanometers.

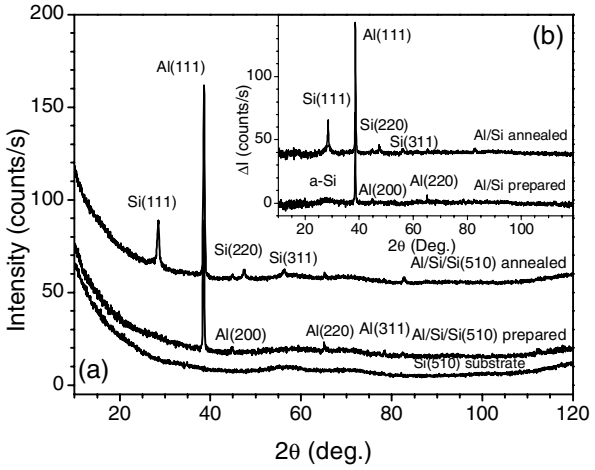

Figure 1. (a) XRD patterns of the prepared and annealed Al/Si bilayers, and of the Si substrate. (b) XRD patterns of the bilayers subtracting the XRD background from the Si(510) substrate.

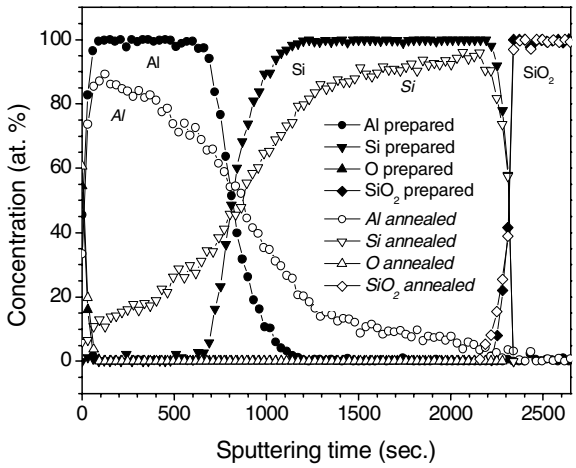

Figure 2. AES depth profiles of the prepared (solid symbols) and annealed (empty symbols) Al/Si/SiO_2/Si(510) bilayers.

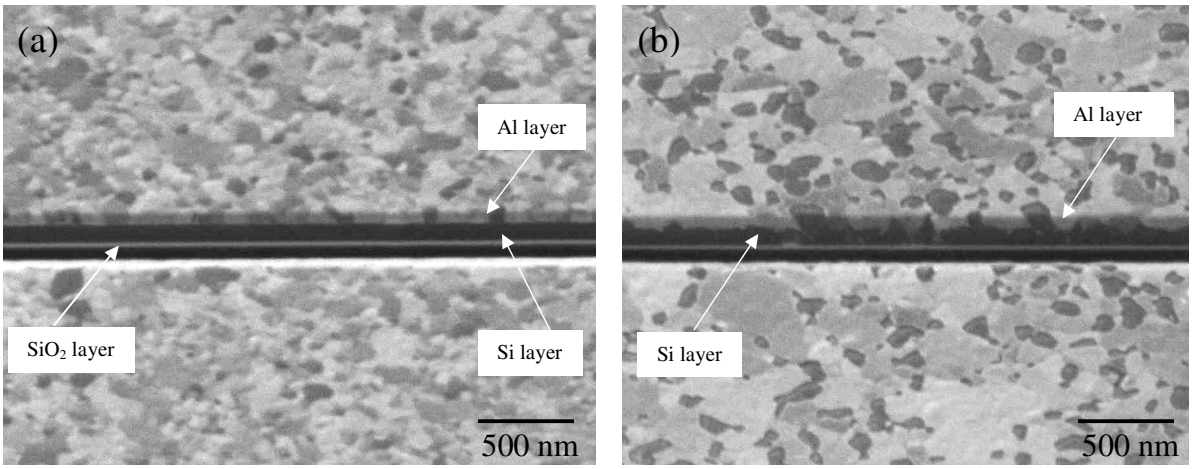

Figure 3. Cross-sectional FIB micrographs for the prepared (a) and annealed (b) Al/Si bilayers.

Figure 4 shows the ψ-dependences of Al {111} peak intensity and the Al {111} pole figures (see the insets) of the prepared and annealed Al/Si bilayers. In both cases, the Al sublayer exhibits a {111} fibre texture. After annealing, the Al {111} texture becomes a little stronger.

For the cubic {111} fibre textured Al and Si thin layers with a (proven by experiment) rotationally symmetric biaxial state of stress parallel to the surface, the lattice strain observed at specimen-tilt angle ψ, ε_ψ, can be related to the stress parallel to the layer surface, σ_l, by [12]:

$$\varepsilon_\psi^{\{111\}} = (2s_{12} + \frac{1}{2}s_{44}\sin^2\Psi + \frac{2}{3}s_0)\sigma_l \qquad (1)$$

where $s_0 = s_{11}\text{-}s_{12}\text{-}s_{44}/2$, with s_{11}, s_{12} and s_{44} as the elastic compliances of the single crystal Al and Si. Hence, a plot of ε_ψ vs $\sin^2\psi$ yields a straight line, and σ_l can be obtained from its slope.

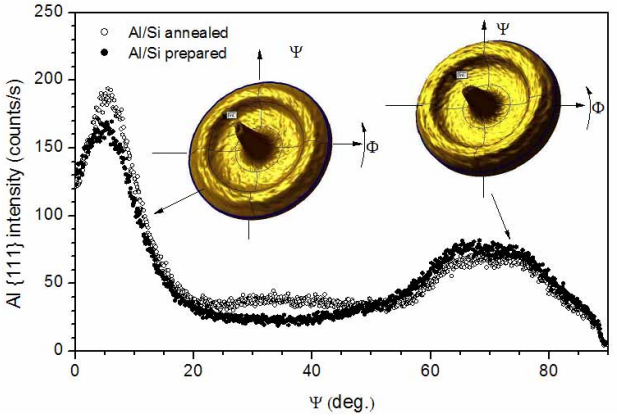

Figure 4. ψ-dependences of Al {111} peak intensity and the Al {111} pole figures (insets) of the prepared and annealed Al/Si bilayers.

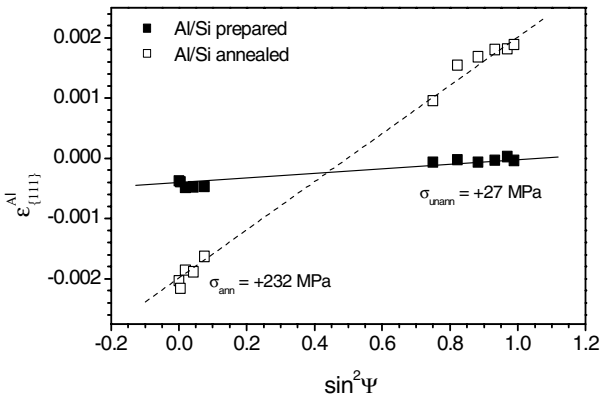

Figure 5. Al {111} lattice strain , $\varepsilon^{Al}_{\{111\}}$, of the prepared and annealed Al/Si bilayers, referred to the lattice spacing of standard Al.

The Al {111} lattice strain, $\varepsilon^{Al}_{\{111\}}$, of the prepared and annealed Al/Si bialyers, with reference to the (strain-free) lattice spacing, $d^{0}_{\{111\}}$, of standard Al powder ($d^{0}_{\{111\}}$ = 2.338 Å), is shown as function of $sin^2\psi$ in figure 5. The measured Al {111} lattice strain vs $\sin^2\psi$ can be well fitted linearly, and the stress parallel to the Al layer can be calculated with s_{11}, s_{12} and s_{44} equal to 16.0 TPa^{-1}, -5.8 TPa^{-1} and 35.3 TPa^{-1}, respectively for single crystal Al [13]. Both Al layers of the deposited and annealed samples possess a tensile stress parallel to the layer surface, and after annealing, the stress of the Al layer has increased from +27 MPa to +232 MPa. For the single crystal Si, s_{11}, s_{12} and s_{44} are 7.74 TPa^{-1}, -2.16 TPa^{-1} and 12.60 TPa^{-1} [13]. Accordingly, the stress parallel to the layer surface in c-Si layer is calculated to be σ_1 = +138 MPa.

The grain size can be determined from both the XRD peak broadening analysis [14] and from the statistical calculation of FIB imaging. Figures 6(a,b) show the statistical lateral grain size distributions of the prepared and annealed Al layers. Each statistical result was calculated from about 1000 crystallites in the FIB top-view images taken at different areas. For the prepared Al layer, the average lateral grain size, *D*, is about 170 nm, and the distribution curve is non-symmetric. After annealing, the average Al grain size increases laterally to 380 nm, and the distribution curve turned to be approximately symmetric shape (figure 6b).

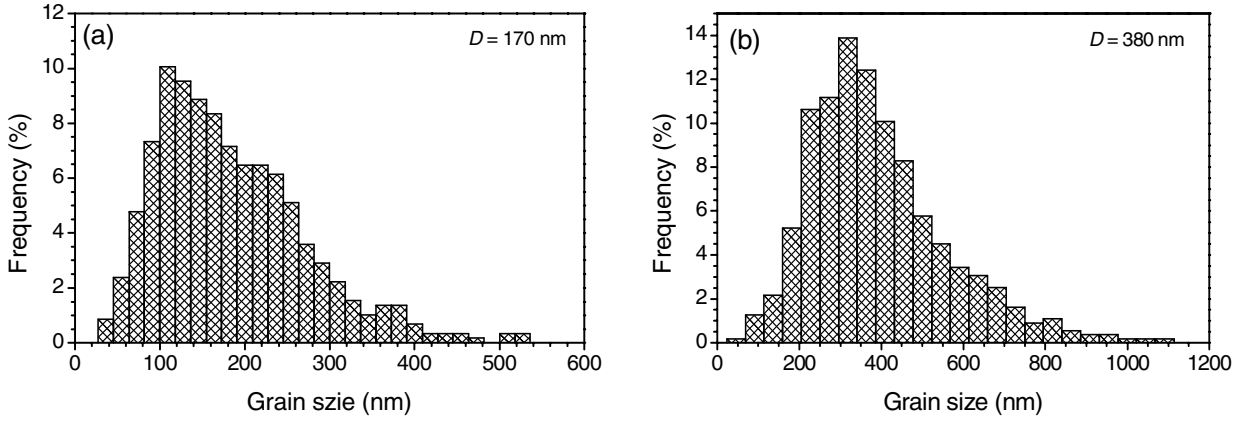

Figure 6. Statistical lateral grain size distributions of prepared (a) and annealed (b) Al sublayers.

The detailed XRD peak broadening analysis was described in Ref. 15. The measured diffraction-line profiles are the convolution of the grain size (often modeled with a Lorentzian function) and/or microstrain (often modeled with a Gaussian function) with the instrumentally broadened profile. Here the instrumental broadening was measured from a coarse-grained Al powder reference sample. On this basis, here the single line Voigt method was used to determine values for the grain size and the microstrain in the direction of the diffraction vector.

The XRD determined grain sizes and the microstrains of the Al (layer) in the as-prepared and annealed Al/Si bilayers are shown in figures 7(a,b) as a function of $\sin^2\psi$ (ψ indicates the direction of the diffraction vector **H**: $\psi = 0°$: **H** is perpendicular to the surface; $\psi = 90°$: **H** is parallel to the surface). For the prepared sample, the Al-grain size along the layer surface ($\psi = 90°$) is about 150 nm, and that along the normal to the layer surface ($\psi = 0°$) is about 95 nm, comparable to the layer thickness. After annealing, the grain grows laterally to about 380 nm and to about 110 nm in the direction perpendicular to the surface. The XRD calculated results agree with those from FIB images. For the prepared Al/Si bilayer, the microstrain along layer surface (0.5 %, $\psi = 90°$) is larger than that along the perpendicular direction to the layer surface (0.4 %, $\psi = 0°$). After annealing, the microstrain in Al along the layer surface has relaxed and an isotropic state of microstrain in the Al layer has been established.

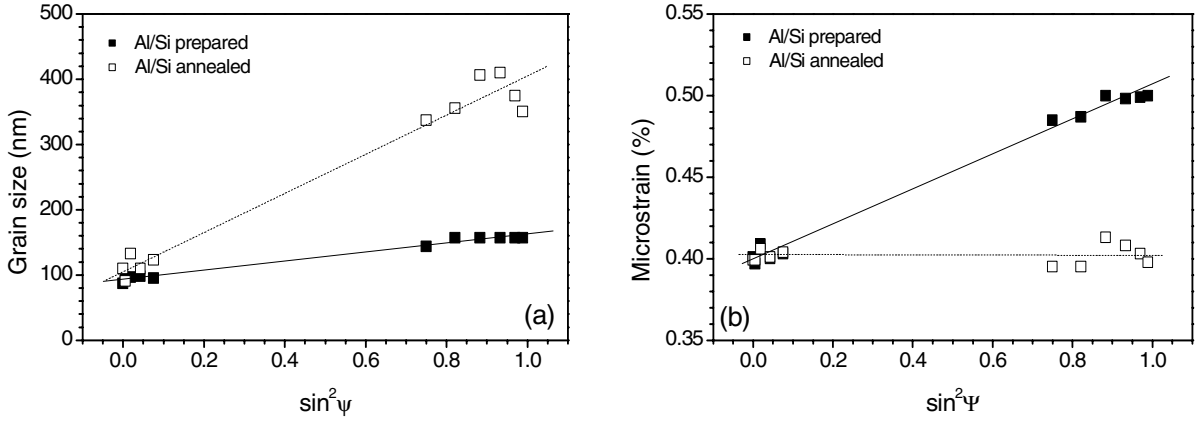

Figure 7. The grain sizes (a) and the microstrains (b) of the Al (layer) in the prepared and annealed Al/Si bilayers

Similarly, the grain size and the microstrain of the c-Si (i.e. after annealing) can be calculated from the broadening of the Si {111} peaks. The crystallite size of the c-Si is very small: it varies from 15 nm perpendicular to the layer surface ($\psi = 0°$) to 10 nm parallel to the layer surface ($\psi = 90°$). The microstrain of the c-Si is about zero both in the parallel and perpendicular directions.

DISCUSSION

At the initial interaction between a-Si and Al sublayers, the c-Si grains nucleate preferentially at the interline of the Al/Si interface and the Al grain boundaries, then grow into the grain boundaries of Al layer, or the Si atoms diffuse into Al grain boundaries and nucleate there followed grain growth (need further experiments), due to the greater ease of reducing free energy at these sites [16]. Besides at the Al grain boundaries, the c-Si grains also nucleate at the Al(crystallites)/Si interface and grow into Al crystallites, forming the wavy interface between the

Si layer and Al crystallites (figure 3b). The later process is much slower than the former one, because the grain boundaries of Al layer are the preferable sites for c-Si nucleation and growth, and the diffusivity of Si atoms along Al grain boundaries is greatly larger that in Al lattice [16].

The growth of c-Si nuclei at the Al grain boundaries developed compressive stress to Al crystallites. This compressive stress makes Al atoms diffuse to the space in the Si layer adjacent to the Al/Si interface, because the original a-Si had moved into the Al layer and left the vacuum space. The diffusion of Al atoms to the Si vacuum space finally made Al crystallites grow into Si layer in a wedged shape (figure 3b). The increased tensile stress of Al layer parallel to the layer surface upon annealing was mainly caused by the thermal stress induced by the cooling process.

CONCLUSION

Upon annealing of an Al/a-Si bilayer at 523 K, the initially substrate adjacent amorphous Si moved into the grain boundaries of the Al layer and crystallized into a {111} textured polycrystal with a crystallite size of approximate 12 nm and a tensile stress of +138 MPa. The initially surface adjacent Al layer grown into the Si layer from the original interface of the Si and Al layers, in association with increases of tensile stress and the lateral grain growth.

REFERENCES

1. S.R. Herd, P. Chaudhari and M.H. Brodsky, J. Non-Cryst. Solids **7**, 309 (1972).
2. G. Ottaviani, D. Sigurd, V. Marrello, J.W. Mayer and J.O. McCaldin, J. Appl. Phys. **45**, 1730 (1974).
3. K. Nakamura, J.O. Olowolafe, S.S. Lau, M-A. Nicolet, J.W. Mayer and R. Shima, J. Appl. Phys. **47**, 1278 (1976).
4. R. Benedictus, A. Böttger and E.J. Mittemeijer, Phys. Rev. B **54**, 9109 (1996).
5. J.L. Murray and A.J. McAlister, Bull. Alloy Phase Diagrams **5**, 74 (1984).
6. F. Oki, Y. Ogawa and Y. Fujiki, Jap. J. Appl. Phys. **8**, 1056 (1969).
7. J.R. Bosnell and U.C. Voisey, Thin Solid Films **6**, 161 (1970).
8. S.R. Herd, P. Chaudhari and M.H. Brodsky, J. Non-Cryst. Solids **7**, 309 (1972).
9. J.K. Toyohiko and S. Robert, Phil. Mag. B **66**, 749 (1992); Mater. Sci. Eng. A **179/180**, 426 (1994).
10. O. Nast, T. Puzzer, L.M. Koschier, A.B. Sproul and S.R. Wenham, Appl. Phys. Lett. **73**, 3214 (1998); O. Nast and S.R. Wenham, J. Appl. Phys. **88**, 124 (2000); O. Nast and A.J. Hartmann, J. Appl. Phys. **88,** 716 (2000).
11. Y.H. Zhao, J.Y. Wang and E.J. Mittemeijer, Thin Solid Films **433**, 82 (2003); Y.H. Zhao, J.Y. Wang and E.J. Mittemeijer, Appl. Phys. A DOI: 10.1007/s00339-003-2247-9 (2003).
12. A.C. Vermeulen, R. Delhez, Th.H. de Keijser and E.J. Mittemeijer, J. Appl. Phys. **77**, 5026 (1995).
13. E.A. Brandes and G.B. Brook, *Smithells Metals Reference Book*, 7th ed. (Butterworth-Heinemann Ltd, Oxford, 1992), p. 15-5.
14. R. Delhez, Th.H. de Keijer and E.J. Mittemeijer, Fres. Z. Anal. Chem. **312**, 1 (1982).
15. D.A. Porter and K.E. Easterling, *Phase Transformations in Metals and Alloys*, 2nd ed. (Chapman and Hall, London, 1992).
16. I. Kaur and W. Gust, *Fundamentals of Grain and Interphase Boundary Diffusion*, 2nd ed. (Ziegler, Stuttgart, 1989).